J. theor. Biol. (2002) **216,** 19–30
doi:10.1006/jtbi.2002.2537, available online at http://www.idealibrary.com on IDEAL®

Robustness as a Measure of Plausibility in Models of Biochemical Networks

MINEO MOROHASHI*†, AMANDA E. WINN‡, MARK T. BORISUK*§, HAMID BOLOURI*‡§‖¶, JOHN DOYLE*§ AND HIROAKI KITANO*§**†‡

** Systems Biology Group Tokyo & Caltech Unit, ERATO Kitano Symbiotic Systems Project, Japan Science and Technology Corporation, M-31 Suite 6A, 6-31-15 Jingumae Shibuya-ku, Tokyo* 150-0001, *Japan, † Department of Fundamental Science and Technology, Keio University, Yokohama* 223-8522, *Japan, ‡ Biocomputation Research Group, Science and Technology Research and Innovation Centre, University of Hertfordshire, Hatfield, AL*10 9*AB, U.K., § Control and Dynamical Systems, California Institute of Technology, Pasadena, CA* 91125, *U.S.A., ‖¶ Division of Biology, California Institute of Technology, Pasadena, CA* 91125, *U.S.A., ** Sony Computer Science Laboratories, Inc.*, 3-14-13 *Higashi-gotanda, Shinagawa-ku, Tokyo* 141-0022 *Japan and ‡† The Systems Biology Institute, Tokyo* 150-0001, *Japan*

(*Received on* 15 *June* 2001, *Accepted in revised form on* 8 *January* 2002)

Theory, experiment, and observation suggest that biochemical networks which are conserved across species are robust to variations in concentrations and kinetic parameters. Here, we exploit this expectation to propose an approach to model building and selection. We represent a model as a mapping from parameter space to behavior space, and utilize bifurcation analysis to study the robustness of each region of steady-state behavior to parameter variations. The hypothesis that potential errors in models will result in parameter sensitivities is tested by analysis of two models of the biochemical oscillator underlying the Xenopus cell cycle. Our analysis successfully identifies known weaknesses in the older model and suggests areas for further investigation in the more recent, more plausible model. It also correctly highlights why the more recent model is more plausible.

Introduction

In recent years, a series of landmark papers have reported the existence of robust behaviors in a variety of biochemical networks (Alon *et al.*, 1999; von Dassow *et al.*, 2000; Yi *et al.*, 2000; Kurata & Taira, 2000). Indeed, robustness in metabolism (Fell, 1997), the cell cycle (Borisuk & Tyson, 1998), and inter-cellular signaling (Freeman, 2000) is now widely accepted. Of course, nothing can be robust to absolutely all variations. Some variations may not matter in terms of the functionality of the system in question. For example, the process that specifies the geometric relationship between hair follicles on human heads need not be very exact or robust. Nor is there any guarantee that all biological systems are necessarily optimally organized. A well-known example of this is the apparently inverted layered structure of the human retina. In this paper, we are interested in robustness to variations in kinetic parameters. That biochemical networks will exhibit robustness to variations in their kinetic parameters was theoretically predicted long ago (Savageau, 1972; Kacser & Burns, 1973). However, these issues

*Author to whom correspondence should be addressed.
E-mail: hbolouri@caltech.edu

0022-5193/02/$35.00/0

have recently received more widespread attention (Dearden & Akam, 2000; Hartwell *et al.*, 1999) due to the growing need to understand the large volumes of data produced by the emerging biotechnologies.

While we tend to think primarily of functionally distinct cellular processes such as metabolism, or the cell cycle, the reality is that all cellular processes are highly interrelated and involve not only biochemical interactions, but also mechanical, electrophysiological, and other interdependencies across multiple time and space scales. Nonetheless, "if we are to comprehend [molecular biology], we must hope that it can be dissected into a series of modules or networks which can be studied in relative isolation" (Dearden & Akam, 2000).

Recent discoveries of modular interspecies conserved networks suggest that such hope may not be in vain. For instance, the InteractiveFly database (http://sdb.bio.purdue.edu/fly/aimain/aadevinx.html) currently lists 36 conserved developmental pathways. The fact that such networks perform homologous functions with similar but differing proteins (hence different reaction rates) and in different cellular contexts (hence different total concentrations of chemical species) suggests functional robustness to such variations.

The chemical oscillator underlying the control of cleavage-stage cell divisions in Xenopus embryos is a well-known example of a robust biochemical module: its component proteins can be replaced by proteins from other species (e.g. human) without affecting its function, and its oscillatory behavior can be reproduced *in vitro* (Murray & Hunt, 1993). In this paper, we compare two models of the Xenopus cell cycle oscillator to evaluate the feasibility of using robustness as a means of identifying potential weaknesses in models. Our approach extends the use of bifurcation analysis for model evaluation by Ringland (1991) and Clarke (1980, 1994) to include observations about the shape, smoothness, and other features of behavior regions in parameter space. The results suggest that the approach can help with iterative development of increasingly detailed models of cellular processes, and selection between alternative explanations (models) of experimentally observed phenomena.

What Should Biochemical Networks be Robust to?

It would be impractical and undesirable for systems to be equally robust to everything. For example, a system *should* be sensitive to particular types of variation in its inputs, otherwise, it would not respond to anything! On the other hand, there is also no reason to believe that all cellular processes will be optimally robust to everything. In this section, we delineate where one can expect robustness or sensitivity and discuss the implications.

To begin, we define a biochemical model as a mapping from parameter space to behavior space. The structure of a network is given by the set of all non-zero elements in its stoichiometry matrix (i.e. the set of interactions in the network). The parameters define reaction kinetics and total (initial) concentrations of the chemical species constituting the modeled network. Two types of parameters may be noted:

(A) Parameters whose values vary during the lifetime of an individual (e.g. temperature, regulated gene activity level, or amount of a protein in a particular state).

(B) Parameters that are constant for individuals, but variable across individuals/species (e.g. reaction rate constants (K_{cat}, K_M), initial/total concentrations).

Any "parameter" that does not vary across individuals or across species is considered a constant here. Inputs are parameters that control the system state trajectory. The inputs to a network can be type A or type B parameters. Sensitivity to type A inputs is useful for behavioral adaptation, while sensitivity to type B inputs can generate diversity in populations without loss of function.

Carison & Doyle (2000) have proposed that robustness to common variations is achieved at the cost of added system complexity. The additional complexity will generally incur some new sensitivities. Optimally robust systems are those that achieve a useful balance between robustness to frequent variations and the concomitant sensitivity to some rare events. A corollary of this view is that natural systems tend to be highly robust to frequently

occurring variations and, in counterbalance, fall catastrophically when some rare variations occur. We exploit this observation to say that if a model of a robust system (e.g. a conserved biochemical network) exhibits sensitivity to a parameter p, one of the following must hold (see also Alves & Savageau, 2000a, b):

(1) p is a control input; in that case the model *should* be sensitive to p. The type of sensitivity will depend on the functionality of the modeled network. Systems that switch between a finite number of states tend to be sensitive to the level of inputs, but not the exact value of any input. On the other hand, systems with continuous outputs (e.g. an amplifier) tend to be sensitive to the exact value of the input(s).

(2) p is regulated (held constant) elsewhere in the system. A familiar example from engineering is power supply provision in electronic circuits: sub-circuits depend critically on receiving a supply voltage held constant by dedicated circuitry. An analogous biochemical example may be the provision of metabolic "services" in cells.

(3) p is not regulated, but the system as a whole is insensitive to p (e.g. soot buildup in a heater will tend to affect heater performance, but not room temperature). In that case, the modeled network is actually a part of a larger system and should be studied in this larger context.

(4) We have misunderstood the function of the network. For example, suppose a system is designed to provide pressure and temperature compensation signals to other systems on an aircraft. We might model the network as only a pressure compensator, and then discover that it is also sensitive to temperature. In such a case, it is not that our model of pressure compensation is wrong, but rather that we have misunderstood the full function of the system.

(5) The model structure is incorrect (e.g. there may be missing components, or incorrect interactions between existing components).

It is often possible to guess whether a model parameter may be a control input from the nature of the processes it controls. For example, the rate of transcription of a gene, the rate of synthesis of a protein, and the initial concentration of a maternally inherited factor are all parameters which are often controlled by upstream biochemical processes and which can usefully control processes such as developmental cell fate specification.

On the other hand, enzyme-mediated reaction rates vary widely among individuals and species (Eanes, 1999), so any biochemical network whose function is conserved across individuals and species may be expected to be highly robust to variations in reaction rates. Similarly, variations in total concentrations of locally synthesized chemical species should not affect the behavior of a structurally correct model dramatically.

When a biochemical model exhibits sensitivity to some of its parameters, one of conditions (1)–(5) above must hold. One may then investigate each possibility in turn. However, sensitivity and robustness are not "all or none", binary characteristics. Below, we define quantitative measures that allow more exact characterization of the type and extent of sensitivity/robustness exhibited. This greater resolution in turn provides greater insight into the potential cause of the observed sensitivity, as illustrated by our example analysis of models of the Xenopus cell cycle.

Measuring Robustness and Sensitivity

Consider an example system with only two parameters $P1$ and $P2$. Suppose the system has a steady state which can be characterized by a single variable, say a concentration level, or an oscillation frequency. Two-parameter bifurcation plots delineate the range of $P1$ and $P2$ for which the system exhibits the measurable behavior. Figure 1 shows two example behavior loci for such a system. The figure is drawn such that the colored regions in (a) and (b) are roughly equal in area. The crosses represent example operating points, that is, the mapping from the particular values of $P1$ and $P2$ to a particular value for the measurable system characteristic. The arrows show the effect of example variations (noise) in $P1$ on the location of the operating

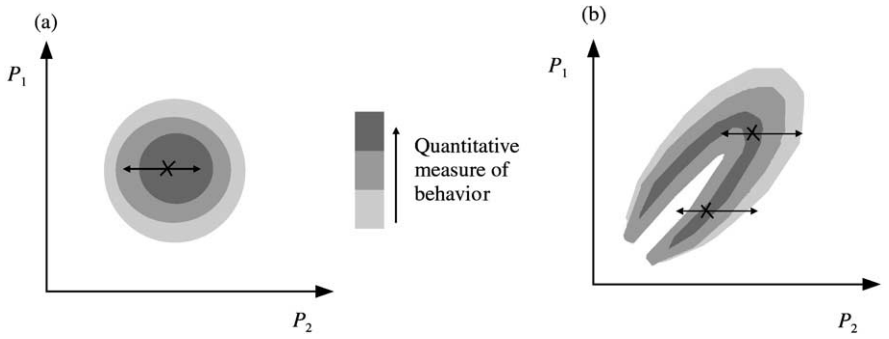

FIG. 1. Schematic representation of two example behavior loci.

point. The model in (a) has two important features:

(1) Define the minimum distance between an operating point and the boundary of the behavior locus as the stability margin (SM) of the operating point. The optimum stability margin (OSM) of the model is then defined as the maximum stability margin achievable by judicious placement of the operating point. The OSM is greater for the convex locus in (a) than for the concave locus in (b). Moreover, the sum of all stability margins is greater for (a) than for (b). Therefore, the model exhibiting characteristic (a) has greater overall stability than the model exhibiting characteristic (b).

(2) For the particular drawings in this example, we note that the rate of change of the measured characteristic with changes in $P2$ is lower in (a) than in parts of (b). Which of the two models is more plausible depends on the extent of behavioral variability observed experimentally.

Where a modeled system exhibits multiple steady state behaviors, there will be one or more loci for each behavior in parameter space and it would be necessary to consider issues such as (1) and (2) (above) for each locus. Often, the multiple behaviors exhibited by a model border each other. Clearly, in such cases convexity of one region would imply concavity in the neighboring region(s). In such cases (as for example in the cell cycle models below), optimum robustness for all model behaviors requires that the boundaries between behavioral regions in parameter space be flat (i.e. neither concave nor convex). The boundaries between neighboring behavior regions are parameter bifurcation loci and can be computed and plotted in two-dimensional slices for visual assessment. For examples, see our cell cycle oscillator analysis below.

For parameters acting as state switch (control) inputs, once a system has switched states, it should be robust to small variations (''noise'') in the input signals, i.e., we require large stability margins for each switched state. Finally, we use Ockham's Razor to distinguish between any two models which may match experimental observations equally well: the model with the greatest parameter robustness—as defined by the above considerations—is the more plausible!

In the remainder of this paper, we explore the above ideas by applying them to two well-known models. Where Ringland (1991) and Clarke (1980, 1994) used bifurcation analysis to obtain models capable of exhibiting experimentally observed steady-state behaviors, we start with models that meet steady-state experimental observations in some qualitative manner (in the examples below, both models produce two cell cycle arrest states and an oscillatory state whose frequency is close to observations). We analyse and compare models on the basis of the size, shape and degree of variability within each steady-state behavior region.

Case Study: The Xenopus Cell Cycle Oscillator

To illustrate and demonstrate the above concepts, we use two models of the cell cycle oscillator that regulates cleavage in early Xenopus embryos (Tyson, 1991; Marlovits *et al.*,

1998). Both models were developed by Tyson and colleagues, and replicate the wild-type *in vivo* and *in vitro* oscillatory behavior and arrest states well. Indeed, at this superficial level they are not distinguishable. The earlier model was essentially theoretical (Tyson, 1991). Its structure is abstract and some interactions within it do not correspond to specific chemical reactions. It was written before experimental data on the structure and kinetics of the system were available. The later model has experimentally validated structure; most of its kinetic parameters have experimentally measured values, and correctly predict the phenotypes of a large range of experimental interventions (Marlovits *et al.*, 1998). With the benefit of hindsight, the limitations of the older model are known. We compare the dynamics of the two models to demonstrate the manner in which robustness analysis can highlight important systematic differences between structurally correct and incorrect models.

WHY USE THE CELL CYCLE AS OUR EXAMPLE CASE STUDY?

The cell cycle oscillator is highly conserved in all eukaryotes (Murray & Hunt, 1993), so there is good reason to believe it is robust to small mutations. There are several additional reasons for our choice.

(1) The basic dynamics observed *in vivo* in Xenopus embryos can also be reproduced *in vitro* using cytoplasmic extracts. There is also no growth during cleavage stages, so growth-directed control of the cell cycle, or other unknown cellular processes are not necessary to explain the fundamental features of the Xenopus cell cycle oscillator.

(2) Xenopus eggs are large and the embryos lend themselves well to experimental analysis. There is therefore a wealth of experimental evidence used by Tyson and colleagues to ensure the plausibility of the more recent structurally detailed model.

(3) Known defects in the earlier model have been experimentally pinpointed.

(4) Analytic solutions of the parameter space are obtainable for the simpler earlier model.

(5) In an extensive study, Borisuk (1997) and Borisuk & Tyson (1998) fully characterized the multidimensional parameter space of the later, more complex model, thus providing unique insights into its behavior as a mapping from parameter space.

OVERVIEW OF THE TWO MODELS

Figure 2 presents an overview of the behavior of cell cycle determinants in Xenopus eggs and embryos. The concentration of an active form of a cyclin–CDC2 dimer—known as the

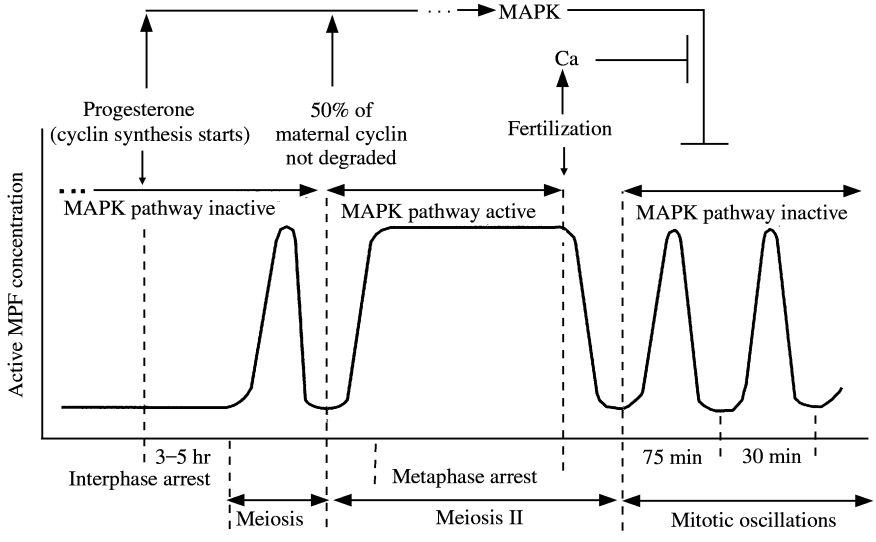

FIG. 2. Schematic representation of some of the major events and mechanisms underlying cellular division in Xenopus eggs and embryos. Note the role of the MAP-kinase-mediated pathway that blocks active MPF degradation (and hence oscillations) until after fertilization (see text for further description).

maturation promoting factor (MPF)—controls cell division activity. The regulation of active MPF concentration is the subject of the two models studied here. Prior to fertilization, active MPF levels are arrested at low concentration in immature eggs and at high concentration in mature eggs. At fertilization, after an initial delay, a series of 12 equal-period, synchronous cell divisions ensue. Thus the system has three steady-state behaviors: low MPF arrest, high MPF arrest, and oscillations in MPF concentration.

Figure 3(a) and (b) are schematic representations of the two models. Both models are based on a cyclic set of reactions involving cyclin–CDC2 dimerization, followed by phosphorylation/dephosphorylatlon and a positive feedback loop which creates hysteretic dynamics. However, the models are otherwise different. In particular, the positive feedback on active MPF is modeled phenomenologically in the '91 model. In the '98 model, on the other hand, the positive feedback loop is defined in terms of a set of specific molecular interactions discussed later and shown in Fig. 10. In addition, the '98 model includes another feedback loop through which active MPF promotes its own degradation. Both of these added structures turn out to have a significant impact on the robustness of the network behavior as discussed below.

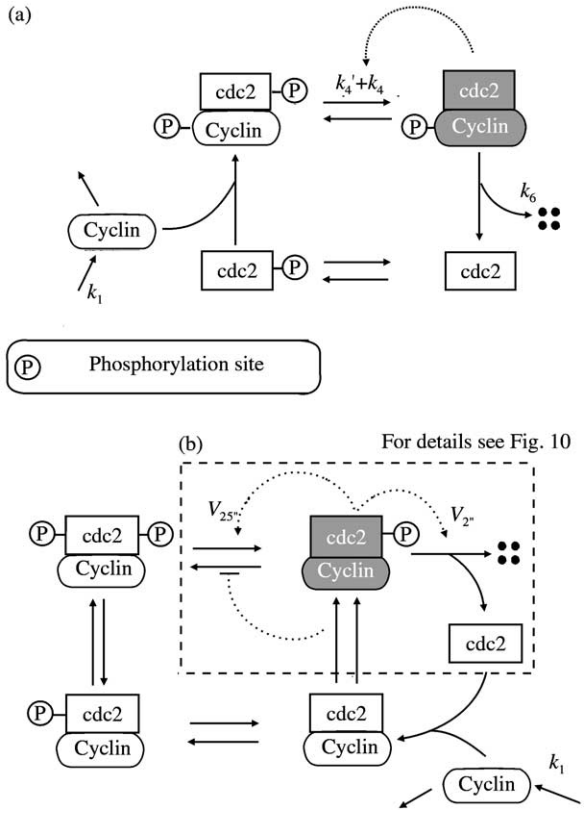

FIG. 3. Schematic representations of the '91 and '98 models of the Xenopus cell cycle oscillator proposed by Tyson and colleagues. Both models share a basic reaction loop in which cyclin dimerization with CDC2 is followed by a series of phosphorylation/dephosphorylation events. (a) The '91 model: at that time, details of the (de)phosphorylation events were not known and were hypothesized. Moreover, the mechanism underlying the positive feedback of active MPF (gray-filled dimer) on its own production was not known and was only modeled phenomenologically. k_1 is the rate of cyclin synthesis. The rate of active MPF formation is modeled as the sum of two components: k_4 is the high rate of active MPF formation proportional to active MPF concentration. k_4' is the low rate of active MPF production proportional to inactive MPF concentration. k_6 is the rate of dimer breakdown. (b) The '98 model: the dimerization and (de)phosphorylation sequence of events have been corrected and the single positive feedback effect of MPF on itself has been replaced by three feedback mechanisms (dotted arrows) each of which is modeled as a set of detailed molecular interactions (see Fig. 10 for details), k_1, V_{25}'', and V_2'' correspond to k_1, k_4 and k_6, respectively, in the '91 model.

CHARACTERISTICS OF THE '91 MODEL

The full '91 model requires six equations and 10 kinetic parameters. But as Tyson showed in 1991, to a good approximation, the model can be reduced to two equations and four kinetic parameters. As illustrated in Fig. 4, the system has three operating regimes corresponding to cell cycle arrests in immature and mature eggs (low and high MPF levels, respectively), and an oscillatory regime corresponding to the cleavage cycles in early embryos. The bifurcation loci between the three behavioral regions can be characterized analytically (see $u_{\mp}$ formulae in Fig. 4). Figure 5(a) and (b) show the variations in the shape and size of these three operating regions as a function of the values of the four kinetic parameters of the system. The surfaces at the boundaries between these regions represent bifurcation loci in parameter space.

Because the reduced '91 model has only four kinetic parameters and is amenable to analytic exploration, we were able to exhaustively plot its behavior in parameter space. As the example in Fig. 5(a) illustrates, the model's three regions of

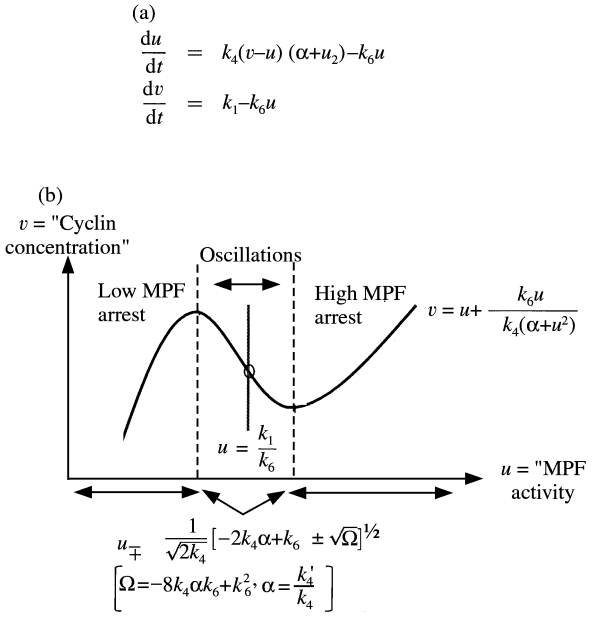

FIG. 4. Overview of the reduced, two-equation version of the '91 model. (a) The two-equation, four-parameter model. (b) Phase portrait of the two-equation model. The v nullcline is a vertical line whose location is given by parameters k_1 and k_6. The u and v nullclines cross only once, giving a single steady state that is either stable (cell cycle arrest states to the left and right of the maximum and minimum of the u nullcline), or unstable (oscillations corresponding to repeated embryonic cell divisions, region between the arrest regions). The loci of the boundaries between these three behavioral regions can be derived analytically from the nullcline equations and are shown below. This allows exhaustive characterization of the model behavior as a function of its four kinetic parameters (see Figs 5 and 6 and text).

steady-state behavior in any two-parameter plot are broad regions with approximately flat boundaries indicating robustness to parameter variations. This is not true for plots involving the rate of cyclin synthesis (k_1). For example, the k_4–k_1 plot in Fig. 5(b) shows that the system behavior depends critically on the value of k_1. Note how changing the value of k_4 affects the choice of k_1 for which the system is in any one particular steady state (seen most readily in the sharp curvature of the boundaries of the oscillating region).

The observation that the system is sensitive to k_1 is not surprising: the oscillatory behavior of the system can be shown to depend on the steady-state concentration of cyclin, which in turn depends on k_1 and k_6. *In vivo*, control of cyclin concentration is achieved through a dual control mechanism consisting of (a) the regulation of cyclin synthesis and (b) the activity of a MAP-kinase-mediated pathway which acts as a binary switch, blocking active-MPF (and hence cyclin) degradation until after fertilization (see Ferrell Jr & Machleder, 1998 and Fig. 2 of this paper). Ferrell Jr *et al.* (1991) and Groisman *et al.* (2000) discuss experimental evidence of the role of cyclin synthesis in the control of the cell cycle. Therefore, we focus on sensitivity to k_1 rather than k_6.

The rate of cyclin synthesis also exerts a strong control on the size of the three regions. With

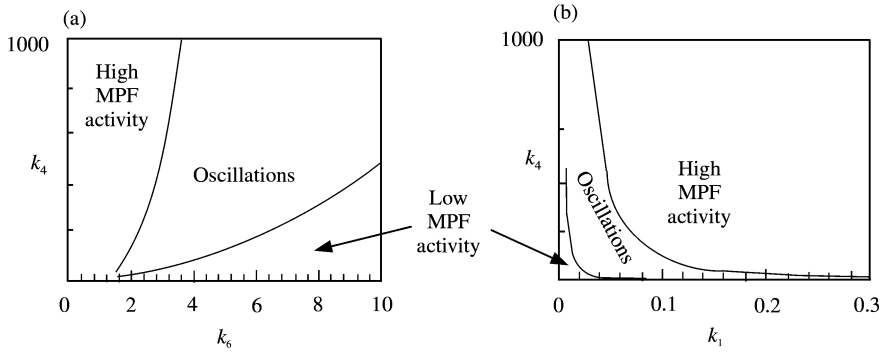

FIG. 5. Two-parameter plots showing the regions in parameter space corresponding to each steady-state behavior of the model. (a) The region between the two curves corresponds to repeated cell divisions in embryos, the area left of this corresponds to the high active-MPF arrest state of mature eggs, and the right hand region to the low active-MPF arrest state of immature eggs. (b) The orientation is reversed. Except for k_4–k_1 plots, as in (b), the characteristics in (a) are typical of all other plots: three approximately equal regions separated by roughly flat boundaries, as would be expected for optimal robustness to parameter variation, (b) demonstrates the nonlinear dependence of system behavior on k_1.

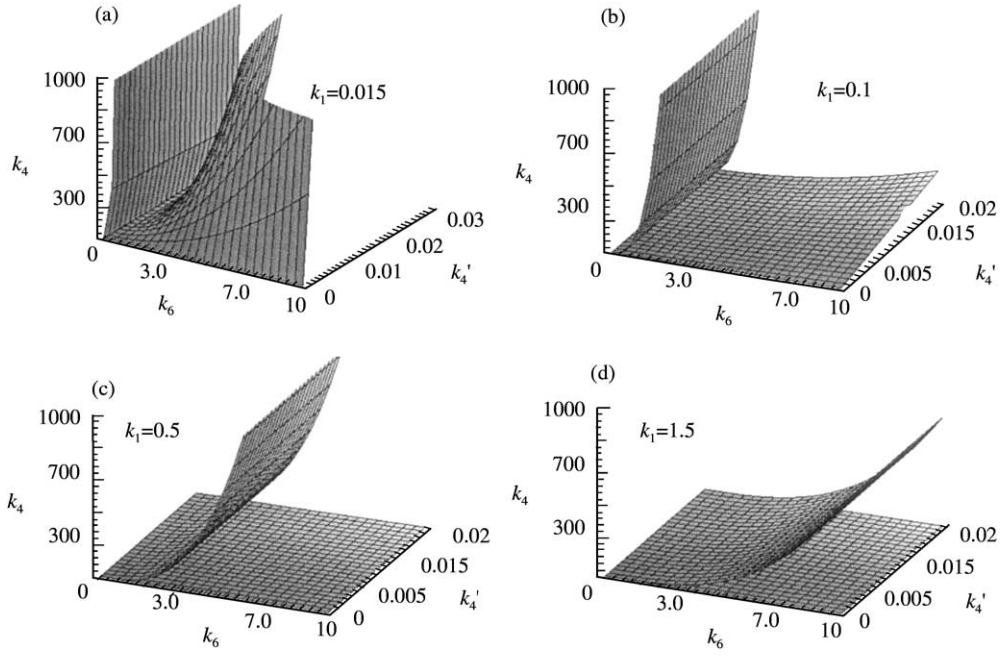

FIG. 6. The effect of varying k_1 on the shape of the model behavior regions in parameter space suggests that the rate of cyclin synthesis may be a state control input for the cell cycle oscillator. (a) For low values of k_1, the region to the right of both planes (low active-MPF immature-egg arrest) occupies most of the volume of the parameter space. So when k_1 (rate of cyclin synthesis) is low, immature egg cell cycle arrest is highly robust to variations (noise) in the values of the other system parameters (k_4, k_4', k_6). (b) For intermediate values of k_1 (here 0.1), the oscillatory region dominates the parameter space and oscillatory behavior is highly robust to changes in the other system parameters. (c) As k_1 is increased further, the size of the region corresponding to high active-MPF mature-egg cell cycle arrest grows. (d) For high values of k_1, the region corresponding to high active-MPF mature-egg cell cycle arrest dominates the parameter space. A cell in this state would be highly robust to variations in the other system parameters.

high values of k_1—Fig. 6(d)—the arrest state for mature eggs dominates. So long as k_1 is high, the system is highly robust to variations in the values of the other three parameters. At the opposite extreme, when k_1 is small—Fig. 6(a)—the size of the regime corresponding to cell cycle arrest in immature eggs is by far the biggest. So with k_1 very small, the immature egg cell cycle arrest state is very robust to variations in the other three kinetic parameters. As the value of k_1 is varied from very low to very high, we see that the size of the middle region (cleavage oscillations) first grows—Fig. 6(b)—and then shrinks again—Fig. 6(c). Figure 6(b) shows an example value for k_1 that results in a very wide oscillatory region occupying most of the parameter space. So with this value, the cell undergoes cleavage oscillations in a manner highly robust to variations in the other three parameters.

It is now known that the Xenopus egg inherits large amounts of maternal cyclin that enables the two meiotic divisions of the egg prior to fertilization. Mitotic oscillations prior to fertilization are prevented by a MAP-kinase-mediated biochemical switch (see the cartoon illustration in Fig. 2 and Ferrell Jr & Machleder, 1998). The sensitivity of the '91 model's behavior to k_1 reveals the role of k_1 as a control input for the mitotic oscillator, acting to generate the capacity for oscillations which are later triggered by fertilization (the biological case for control of the embryonic cell cycle by cyclin synthesis was first put forward by Murray & Kirschner (1989) and Murray *et al.* (1989). The nonlinear (k_4-related) dependence of the system behavior on k_1 reveals a weakness in the model: the state of the system cannot be predicted from the value of the control input (k_1) alone.

Note that in Fig. 6, k_4 ranges from 0 to 1000. To be comparable to the experimentally measured values of the corresponding parameters used in the '98 model, k_4 should be limited

to <10. However, if we limit the value of k_4 to this smaller range, the robust model behavior observed in Fig. 6 can only be replicated if k_1 is increased to values beyond its plausible range (here taken as nominal $\pm$ one order of magnitude). Thus, with the benefit of hindsight, we note that the structural weakness of a single (phenomenological) feedback loop in the '91 model results in a need for unfeasibly large parameter ranges in the model.

Figure 7 is a plot of the oscillation frequency of the model as a function of parameters k_1 and k_4. As expected, the oscillation frequency is zero in the dark-blue regions corresponding to the two cell cycle arrest states discussed above (low-MPF immature-egg arrest to the left, high-MPF mature-egg arrest to the right). In the region in between these, the value of k_1 determines the cleavage oscillation frequency. The values of the other parameters are set to those recommended in Tyson (1991). The period of the resulting oscillations ranges from 10 to 50 min. The *in vivo* period for Xenopus cleavage cycles is 30 min (Masui & Wang, 1998). The *in vitro* period is around 60 minutes (Murray & Hunt, 1993). So the model includes the observed *in vivo* and *in vitro* behaviors, but its exact oscillation period varies with changes in k_1. Since k_1—the protein synthesis rate—cannot be controlled very tightly *in vivo*, this sensitivity suggests that the model has structural deficiencies.

It is possible to optimize the model parameters to constrain the frequency range of the oscillatory region. However, in this case the oscillatory region becomes very narrow and the sensitivity of the model to k_1 variations is even more pronounced. As we show below, the '98 model does not suffer from this problem.

CHARACTERISTICS OF THE '98 MODEL

The full '98 model is represented by nine differential equations and 26 kinetic parameters. It is clearly far too complicated to study analytically. We used the numerical bifurcation analysis tool AUTO (Doedel, 1981) to characterize this model in the same manner as the '91 model. Based on the earlier results of Borisuk & Tyson (1998), we knew that the model has robustness characteristics similar to the '91 model, and that k_1 continues to control system state. Figure 8(a) and (b) illustrate this point. In Fig. 8(a), k_1 is set to a high value (corresponding to large amounts of maternal cyclin being present in the egg in which the degradation of cyclin is blocked by the MAP kinase pathway) and we see that virtually all of the plausible parameter space (the volume to the left of the plotted surface) is taken up by the region corresponding to high-MPF cell cycle arrest in mature eggs. In Fig. 8(b), k_1 is reduced to 0.01 (corresponding to fertilized eggs, where the MAP kinase pathway is disabled and maternal cyclin has been degraded), and we see that now the same volume in parameter space represents oscillatory behavior (the volume between the

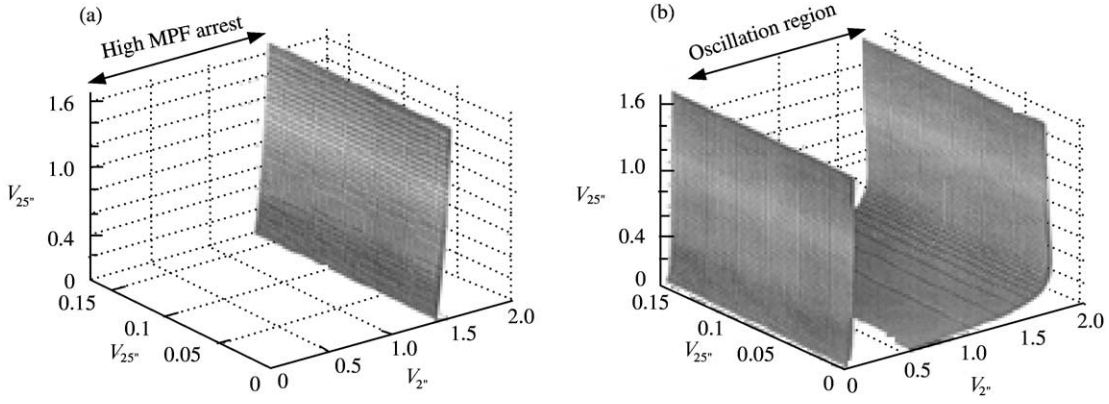

FIG. 8. The effect of varying k_1 on the size and shape of the behavior regions in the '98 model parameter space. The flat, nearly vertical surfaces separating the regions are close to the ideal for optimum robustness to variations in the other system parameters. Compared to the corresponding characteristics in the '91 model (Fig. 6), the '98 regions are also much larger, thus offering greater robustness. The values of k_1 are (a) 1.0, and (b) 0.01, respectively.

two surfaces). Note that the above state control characteristic of k_1 is highly robust to variations in other kinetic parameters: changes in V''_{25}, V'_{25}, and V''_2 (corresponding to k_4, k'_4 and k_6 in the '91 model, respectively, see Fig. 3) have virtually no effect on this behavior.

A critical difference between the '91 and '98 models is that the period of oscillations is much less variable in the '98 model. In the latter, the value of k_1 determines whether the system oscillates. However, the period of oscillations is fixed by the combination of the values of the other parameters in the system. Since these parameters would be expected to be constant in any individual, the cleavage period would be fixed and not vary with small fluctuations in the regulated value of k_1. In a sense, k_1 control behaves like a multi-level switch. Its value is interpreted in three discrete levels: low, medium and high. These in turn determine the mode of operation of the cell cycle engine. In comparison with the '91 model, the '98 model is not only less sensitive to parameters other than k_1, but also operates with greater stability margins on k_1.

As shown in Fig. 9, the parameter values of the '98 model—which are based on *in vitro* experimental measurements—result in 45–50 min period oscillations similar to *in vitro* preparations. Note, however, the existence of a triangular region of frequency instability where k_1 is small. Moreover, the range of k_1 values for which the system oscillates seemed surprisingly small to us. On further investigation, we found that the positive feedback loop through which MPF facilitates its own degradation (shown in Fig. 10(b)) is not experimentally specified. Moreover, Tyson and colleagues did not optimize the parameters of these reactions for any particular behavior, but rather used nominal values. As shown in Fig. 11, optimizing these unknown parameters for oscillation periods in the *in vitro* range dramatically improves the robustness characteristics of the '98 model. The oscillatory region is now much wider than that of the '91 model. The oscillation period is remarkably constant, and k_1 control of cell state no longer depends on co-variation with other rates (V''_{25} in the '98 model corresponds to k_4 in the '91 model). Thus, robustness analysis of the

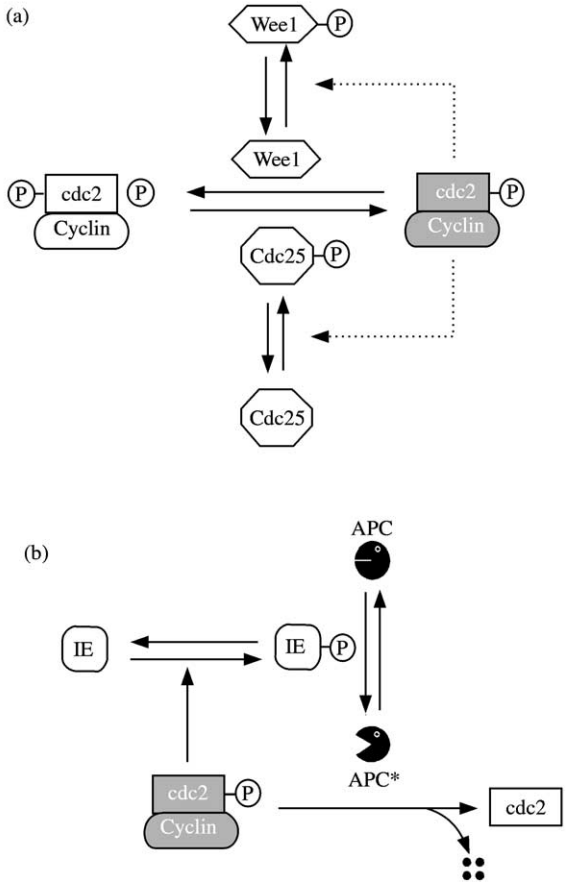

FIG. 10. Details of the additional reactions included in the '98 model. (a) The push–pull positive feedback mechanisms replacing the simple phenomenological feedback of active-MPF on itself in the '91 model. The CDC25 path enhances the rate of active-MPF production while the wee1 path reduces the rate of return of active-MPF (gray-filled dimer) to inactive form. (b) The feedback mechanism of active-MPF on its own degradation. APC is the anaphase promoting factor, and its role in active MPF degradation has been experimentally verified. But intermediate enzyme (IE) has not been experimentally identified and its interactions represent only an abstract path.

'98 model not only highlighted a potential weakness in the model, but also pinpointed where the problem may lie and allowed us to remedy it.

Although we have shown that the structure of the '98 model is capable of providing highly robust oscillatory behavior in a manner far exceeding the capabilities of the '91 model, it cannot be assumed that the '98 model is a complete representation of all the pertinent interactions constituting the Xenopus cell cycle oscillator. The structure of the '98 model is

clearly more plausible than the '91 model, but it could be further optimized. For example, Fig. 12 shows that increasing the autocatalytic rate of active MPF degradation can enlarge the oscillatory region of the model considerably. The structure of the '98 model ensures that the expanded oscillatory region has a very stable period (in Fig. 12 optimized to lie in the range 28 to 30 minutes corresponding to *in vivo* oscillations). Moreover, there is no co-dependence on parameters other than k_1. Experimental data only put a lower bound on the value of the parameter optimized here (V_2''). The exact *in vivo* value is not known. Nor is it significant for our purposes. The important observation here is that more detailed modeling of this particular part of the model may be illuminating.

Discussion and Conclusions

Model building necessarily involves making choices between alternative explanations with apparently equivalent behaviors. We put forward an argument from first principles suggesting that robustness analysis can help distinguish between more and less plausible models, and pinpoint structural weaknesses in models. The proposal is predicated on the expectation that essential cellular processes that are conserved across multiple species must be functionally robust to mutational variations. Our analysis of two models of the Xenopus cell cycle oscillator confirms this theoretical expectation, but further examples are needed.

Our choice of models for this paper was highly serendipitous. The parameter space of the more complex '98 model had already been mapped in great detail by Borisuk (1997). We could thus concentrate on comparing the two models rather than characterizing each in detail first. Efficient characterization of the parameter space of models with tens of parameters is a significant remaining challenge. Recently, fairly general relaxation methods that exploit linear matrix inequalities to simplify the searching of multi-dimensional spaces have been developed (Parrilo, 2000). We hope to exploit these developments to facilitate characterization and parameter searching in future applications of our approach to model building and validation.

Methods

The analytical solution of the parameter space for the two-equation version of the 1991 model was derived using Waterloo Maple (http://www.maplesoft.com/). All other numerical characterizations of the parameter spaces of the two models were performed using the AUTO bifurcation analysis package (http://indy.cs.concordia.ca/auto/main.html). The frequency contour plots were generated as co-dimension two-bifurcation plots on which the frequency of oscillation was superimposed post hoc. Oscillation frequencies were calculated by sampling the oscillatory region of each plot in a 100×100 or a 50×50 grid, grouping the results into bins, and then using the AUTO to trace the loci of each frequency bin. Numerical parameter optimizations were carried out interactively using Berkeley Madonna (http://www.berkeleymadonna.com/).

We are grateful to Drs John Tyson and Kathy Chen for much help and advice and to Drs Baltazar Aguda, Maria Schilstra, and Herbert Sauro for helpful critical reviews of the manuscript.

REFERENCES

Alon, U., Surette, M. G., Barkai, N. & Leibler, S. (1999). Robustness in bacterial chemotaxis. *Nature* **397,** 168–171.

Alves, R. & Savageau, M. A. (2000a). Comparing systemic properties of ensembles of biological networks by graphical and statistical methods *Bioinformatics* **16,** 527–533.

Alves, R. & Savageau, M. A. (2000b). Systemic properties of ensembles of metabolic networks: application of graphical and statistical methods to simple unbranched pathways. *Bioinformatics* **16,** 534–547.

Borisuk, M. T. (1997). Ph.D. Thesis, Department of Mathematics, Virginia Polytechnic Institute and State University.

Borisuk, M. T. & Tyson, J. J. (1998). Bifurcation analysis of a model of mitotic control in frog eggs. *J. theor. Biol.* **195,** 69–85.

Carlson, J. M. & Doyle, J. (2000). Highly optimized tolerance: robustness and design in complex systems. *Phys. Rev. Lett.* **84**, 2529–2532.

Clarke, B. L. (1980). Stability of complex reaction networks. In: *Advances in Chemical Physics* (Prigogine, I. & Rice, S. A., eds), pp. 1–215. New York: John Wiley.

Clarke, B. L. (1994). Steady state bifurcation hypersurfaces of chemical mechanisms. In: *Comparison Methods and Stability Theory*, *Lecture Notes in Pure and Applied Mathematics* (Segel, D. & Liu, X., eds), Vol. 162, pp. 67–85. New York: Marcel Dekker.

Dearden, P. & Akam, M. (2000). Segmentation in silico. *Nature* **406,** 131–132.

Doedel, E. J. (1981). AUTO: a program for the automatic bifurcation analysis of autonomous systems. *Proceedings of the* 10*th Manitoba Conference on Numerical Mathematics and Computers*, Winnipeg, Canada, pp. 265–284.

Eanes, W. F. (1999). Analysis of selection on enzyme polymorphisms. *Annu. Rev. Ecol. Syst.* **30,** 301–326.

Fell, D. A. (1997). *Understanding the Control of Metabolism*. London: Portland Press.

Ferrell Jr, J. E. & Machleder, E. M. (1998). The biochemical basis of an all-or-none cell fate switch in Xenopus oocytes. **280,** 895–898.

Ferrell Jr, J. E., Wu, M., Gerhardt, J. C. & Martin, G. S. (1991). Cell cycle tyrosine phosphorylation of p34cdc2 and MAP-kinase homolog in Xenopus oocytes and eggs. *Mol. Cell. Biol.* **11,** 1965–1971.

Freeman, M. (2000). Feedback control of intercellular signalling in development. *Nature* **408,** 313–319.

Groisman, I., Huang, Y.-S., Mendez, R., Cao, Q., Theurkauf, W. & Richter, J. D. (2000). CPEB, maskin, and cyclin B1 mRNA at the mitotic apparatus: implications for local translational control of cell division. *Cell* **103,** 435–447.

Hartwell, L. H., Hopfield, J. J., Leibler, S. & Murray, A. W. (1999). From molecular to modular biology. *Nature* **402,** C47–C52.

Kacser, H. & Burns, J. A. (1973). The control of flux. *Symp. Soc. Exp. Biol.* **27,** 65–104.

Kurata, H. & Taira, K. (2000). Systematic analysis of the robustness in complex reaction networks of bacteria. *Proceedings of the Fourth Annual International Conference on Computational Molecular Biology*, Tokyo, Japan, pp. 36–37

Marlovits, G., Tyson, C. J., Novak, B. & Tyson, J. J. (1998). Mathematical model of the fission yeast cell cycle with checkpoint controls at the G1/S, G2/M and metaphase/anaphase transitions. *Biophys. Chem.* **72,** 169–184.

Masui, Y. & Wang, P. (1998). Cell cycle transition in early embryonic development of Xenopus leavis. *Biol. Cell* **90,** 537–548.

Murray, A. & Hunt, T. (1993). *The Cell Cycle*. London: Oxford University Press.

Murray, A. W. & Kirschner, M. W. (1989). Cyclin synthesis drives the early embryonic cell cycle. *Nature* **339,** 275–280.

Murray, A. W., Solomon, M. J. & Kirschner, M. W. (1989). The role of cyclin synthesis and degradation in the control of maturation promoting factor activity. *Nature* **339,** 280–286.

Parrilo, P. A. (2000). Control and dynamical systems. Ph.D. Thesis, California Institute of Technology.

Ringland, J. (1991). Rapid reconnaissance of a model of a chemical oscillator by numerical continuation of a bifurcation feature of codimension 2. *J. Chem. Phys.* **95,** 555–562.

Savageau, M. A. (1972). The behavior of intact biochemical control systems. *Curr. Topics Cellular Regulation* **6,** 63–130.

Tyson, J. J. (1991). Modeling the cell division cycle: cdc2 and cyclin interactions. *Proc. Natl Acad. Sci. U.S.A.* **88,** 7328–7332.

von Dassow, G., Mier, E., Munro, M. & Odell, M. (2000). The segment polarity network is a robust developmental module. *Nature* **406,** 188–192.

Yi, T.-M., Huang, Y., Simon, M. I. & Doyle, J. (2000). Robust perfect adaptation in bacterial chemotaxis through integral feedback control. *Proc. Natl Acad. Sci. U.S.A.* **97,** 4649–4653.

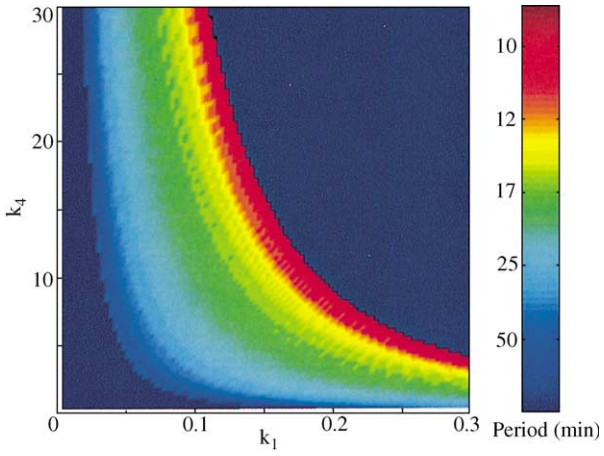

FIG. 7. Contour plot of the frequency of cleavage oscillations in the '91 model. According to this model, the cleavage period would vary between 10 and 50 min from individual to individual, even when all "environmental conditions" are held constant. This contradicts experimental observations of a stereotypic cell division period in Xenopus embryos.

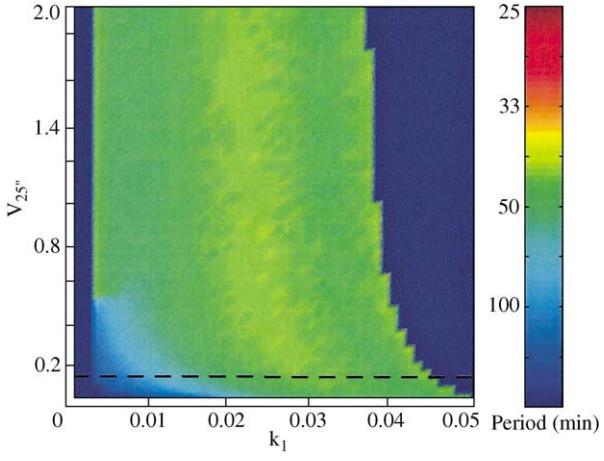

FIG. 9. Cleavage frequency contour plot using the Mariovits *et al.* parameter values for the '98 model. Note that the oscillatory region is very narrow, but has the advantage of a much more stable oscillation period range (45–50 min) in most of the oscillatory region. The dashed horizontal line indicates the experimentally derived value of V_{25}'' used by Mariovits *et al*. In this region of the parameter space, the oscillation period ranges from 50 down to 10 min, thus negating the apparent greater stability of the '98 model.

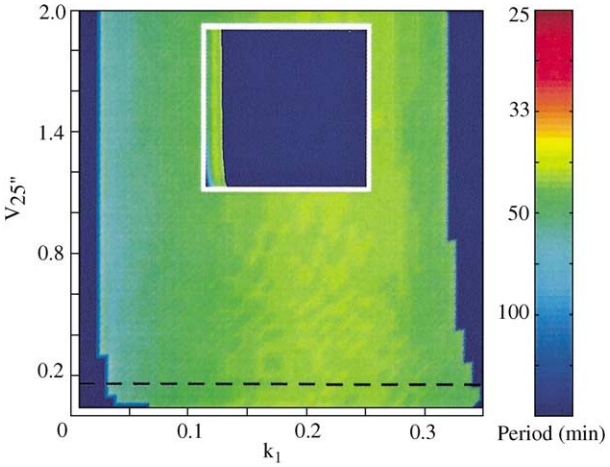

FIG. 11. The '98 model optimized to give *in vitro* like oscillations. The period is highly stable across the whole region, ranging between 45 and 65 min. Note also the nearly vertical boundaries of the oscillatory region: k_1 can control state transition without codependence on other parameters (V_{25}'' plotted, but similar for others). The width of the oscillatory region (and hence the operational stability margin) is also considerably wider than for the '91 model. The IE-related parameters for which experimental data were not available and have been optimized here are: $k_{le} = 1.2$, $k_{mie} = 0.006$, $k_{ier} = 0.7$, $k_{mier} = 0.001$, $k_{map} = 1$, $k_{apr} = 0.11$, $k_{mapr} = 4$ (symbols correspond to the notation of (25)).

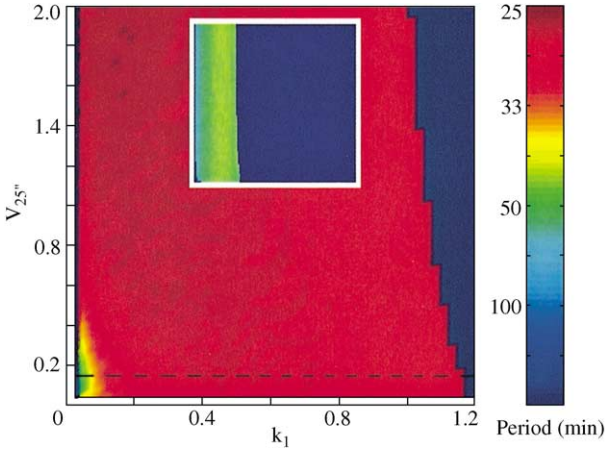

FIG. 12. The '98 model optimized to give robust *in vivo* like oscillations. This particular plot was obtained by simply increasing V_2''—the fast rate of degradation of active-MPF by APC—to 1.5 min^{-1}. V_2'' corresponds to k_6 in the '91 model. As shown in Fig. 4(d), increasing k_6 has a similar effect on the '91 model. But whereas in the '91 model the period of oscillations varies widely across the region, in the optimized '98 model the period is highly stable in the range 28–30 min. Note that the Marlovits *et al.* choice of $V_2'' = 0.25\ \text{min}^{-1}$ was based on experimental evidence that suggests a lower limit on V_2'' but no specific upper limit.

doi: 10:1006/jtbi2002.2537